Supplement of Atmos. Chem. Phys., 18, 12595–12612, 2018
https://doi.org/10.5194/acp-18-12595-2018-supplement

Atmospheric Chemistry and Physics
Open Access
EGU

Supplement of

The diverse chemical mixing state of aerosol particles in the southeastern United States

Amy L. Bondy et al.

Correspondence to: Andrew P. Ault (aulta@umich.edu)

1 SEARCH network $PM_{2.5}$ and meteorological measurements

The SouthEastern Aerosol Research and Characterization Network (SEARCH) is a multi-pollutant network designed to address regulatory and scientific questions related to ozone and its precursors, particulate matter mass and composition, and atmospheric visibility in addition to other research concerns. Active since 1992, Centreville, AL is one of a handful of sites that is part of SEARCH. During SOAS, meteorological conditions including wind direction, wind speed, solar radiation, precipitation, and relative humidity were monitored from the SEARCH network, plotted in Figure S1. Additionally, the network also collected and determined mass concentrations of EC, NH_4^+, NO_3^-, OC, SO_4^{2-}, and $PM_{2.5}$ (using a tapered element oscillating microbalance, TEOM) shown in Figure 1. The box green boxes overlaid on the meteorological data in Figure S1 identify the two SOA-rich time periods. Similarly, tan boxes indicate the dust-rich time periods and blue boxes the SSA-rich time periods which were analyzed in this study.

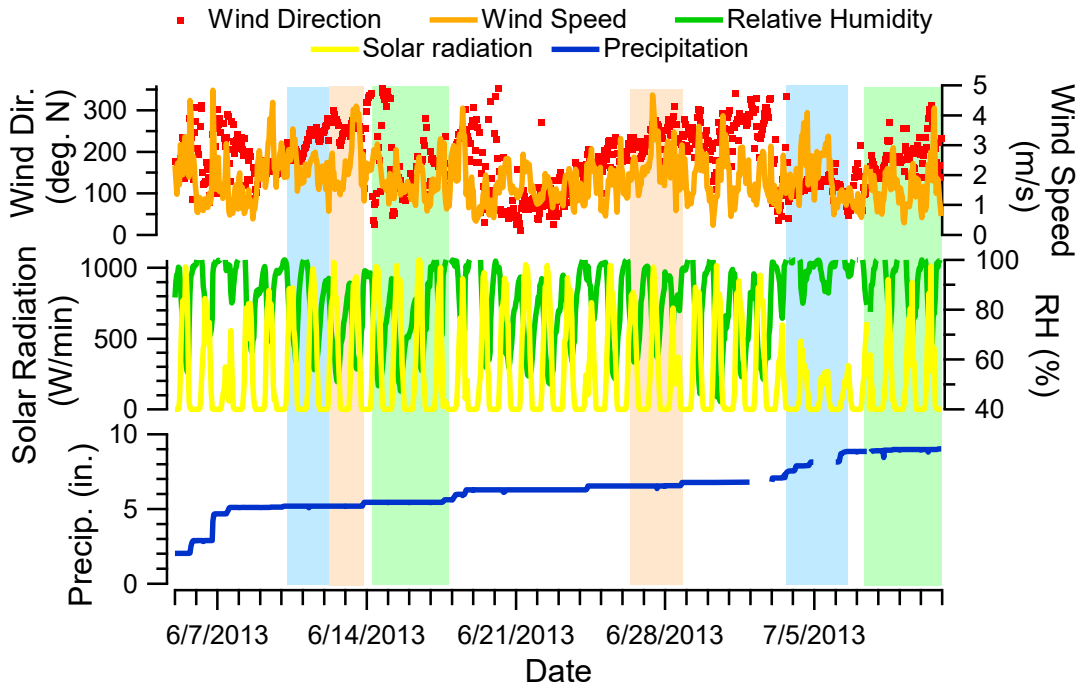

Figure S1. SEARCH meteorological data for Centreville, AL during SOAS with green boxes overlaid for the two SOA-rich time periods, tan boxes for the dust-rich time periods, and blue boxes overlaid for the SSA-rich time periods.

2 CCSEM-EDX analysis

SOAS intensive time periods, selected based on meteorological conditions, had shorter MOUDI collection times (3 hours rather than 11 hours.) The intensive dates are shown in Table S1 below, with the sample times highlighted in blue showing periods where CCSEM-EDX was run.

Table S1. Intensive sample collection times. Highlighted samples were analyzed using CCSEM-EDX.

Intensive Date	Time (CST)
6/10/13	8:00-11:00
6/10/13	12:00-15:00
6/10/13	16:00-19:00
6/10/13	20:00-7:00
6/11/13	8:00-11:00
6/11/13	12:00-15:00
6/11/13	16:00-19:00
6/11/13	20:00-7:00
6/12/13	8:00-11:00
6/12/13	12:00-15:00
6/12/13	16:00-19:00
6/12/13	20:00-7:00
6/14/13	8:00-11:00
6/14/13	12:00-15:00
6/14/13	16:00-19:00
6/14/13	20:00-7:00
6/15/13	8:00-11:00
6/15/13	12:00-15:00
6/15/13	16:00-19:00
6/15/13	20:00-7:00
6/16/13	8:00-11:00
6/16/13	12:00-15:00
6/16/13	16:00-19:00
6/16/13	20:00-7:00
6/29/13	8:00-11:00
6/29/13	12:00-15:00
6/29/13	16:00-19:00
6/29/13	20:00-7:00
6/30/13	8:00-11:00
6/30/13	12:00-15:00
6/30/13	16:00-19:00
6/30/13	20:00-7:00
7/1/13	8:00-11:00
7/1/13	12:00-15:00
7/1/13	16:00-19:00
7/1/13	20:00-7:00
7/9/13	8:00-11:00
7/9/13	12:00-15:00
7/9/13	16:00-19:00
7/9/13	20:00-7:00

All sampling periods that were analyzed using CCSEM-EDX are indicated in Table S2 below. The MOUDI stage(s) that were analyzed, in addition to the number of particles per sample, are also indicated. The aerodynamic diameter 50% cut points, detailed in Marple et al (1991), are as follows: stage 5 (1.8 μm), stage 6 (1.00 μm), stage 7 (0.56 μm), stage 8 (0.32 μm), stage 9 (0.18 μm), stage 10 (0.100 μm), and stage 11 (0.056 μm). Not every sample collected was analyzed due to time/funding constraints and damaged substrates.

Table S2. Sampling times of all CCSEM-analyzed MOUDI samples and the number of particles analyzed per stage.

Sample Date	Time (CST)	Stage(s)	# of particles
6/5/13	10:00-19:00	7	145
6/6/13	20:00-7:00	6 / 7	23 / 43
6/7/13	8:00-19:00	7	305
6/7/13	20:00-7:00	6	222
6/8/13	8:00-19:00	6	167
6/10/13	8:00-11:00	6 / 8	395 / 580
6/10/13	12:00-15:00	6 / 8	518 / 497
6/10/13	16:00-19:00	8	281
6/10/13	20:00-7:00	7	567
6/11/13	8:00-11:00	7	431
6/11/13	16:00-19:00	7	450
6/11/13	20:00-7:00	7	553
6/12/13	8:00-11:00	6 / 8	305 / 151
6/12/13	12:00-15:00	5 / 7 / 8	129 / 474 / 1314
6/12/13	16:00-19:00	6 / 7	365 / 220
6/12/13	20:00-7:00	7 / 9	581 / 2313
6/13/13	8:00-19:00	5 / 8 / 10	462 / 653 / 688
6/13/13	20:00-7:00	7	122
6/14/13	8:00-11:00	6 / 7	101 / 355
6/14/13	12:00-15:00	6 / 7 / 8	22 / 343 / 402
6/14/13	16:00-19:00	8	512
6/14/13	20:00-7:00	6	100
6/15/13	8:00-11:00	7 / 8	384 / 380
6/15/13	20:00-7:00	6 / 7 / 8	84 / 532 / 2304
6/16/13	8:00-11:00	7	239
6/16/13	16:00-19:00	7	338
6/16/13	20:00-7:00	6 / 8	514 / 791
6/17/13	8:00-19:00	7	2707
6/20/13	8:00-19:00	6 / 7	134 / 938
6/26/13	20:00-7:00	6 / 7	295 / 539
6/28/13	20:00-7:00	7	95
7/1/13	12:00-15:00	7	392
7/3/13	20:00-7:00	7	711
7/4/13	8:00-19:00	7	1826
7/5/13	8:00-19:00	7	448
7/6/13	8:00-19:00	6 / 10 / 11	369 / 64 / 342
7/7/13	8:00-19:00	7 / 10	209 / 690
7/7/13	20:00-7:00	9	153
7/8/13	8:00-19:00	6 / 9 / 11	137 / 755 / 1246
7/8/13	20:00-7:00	9	260
7/9/13	16:00-19:00	5 / 6 / 10 / 11	527 / 446 / 846 / 879
7/11/13	8:00-19:00	9	1262

3 Calculation of particle volume equivalent diameters

To describe the impact of size on aerosol chemical diversity during SOAS, projected area diameters (D_{pa}) measured using CCSEM-EDX were converted to volume equivalent diameters (D_{ve}) using a conversion factor determined from atomic force microscopy (AFM) height images of organic particles from SOAS collected on silicon substrates (Ted Pella Inc.). As particles can undergo spreading upon impaction on substrates, D_{ve} represents the size of particles before impaction. AFM images from organic aerosol particles collected during SOAS on June 14, 2013 were used in the subsequent analysis to calculate a conversion factor between D_{pa} and D_{ve} for SOA and biomass burning particles. As SSA during SOAS was predominately aged by HNO_3 leading to $NaNO_3$ in the particle phase (Bondy et al., 2017b), a SSA spreading conversion factor was calculated using laboratory-generated $NaNO_3$ (Bondy et al., 2017a). Though organic aerosol particles and SSA are expected to spread upon impaction as they are generally liquids at the temperatures and relative humidities presented, mineral dust, fly ash and primary biological particles are not expected to spread as they are solid. Thus, D_{pa} is equivalent to D_{ve} for mineral dust, fly ash and biological particles.

AFM was performed on a nanoIR2 system (Anasys Instruments). AFM height/deflection images were collected in contact mode (IR power 21.27%, filter in) at a scan rate of 1 Hz using a gold-coated contact mode silicon nitride probe (Anasys Instruments, 13 ± 4 kHz resonant frequency, 0.07-0.4 N/m spring constant). Volumes of particles were measured using SPIP software (v6.2.6, Image Metrology, Hørsholm, Denmark), and from these volumes, D_{ve} was calculated for each particle. Table S3 shows the measured height and diameter, calculated volume, and calculated D_{ve} for select organic particles from SOAS (~100 particles were actually used to calculate the conversion factor). From these results, SOA and biomass burning particles were multiplied by a conversion factor of 0.49 to convert D_{pa} to D_{ve}.

Table S3. AFM-measured and volume-calculated diameters of organic aerosol collected during SOAS on June 14, 2013. *Note, the physical characteristics of ~100 particles were analyzed in the volume calculations, however only a fraction are shown here for brevity.

Particle #	D_{pa} (nm)	Height (nm)	Volume (nm^3)	D_{ve} (nm)
1	437	61	6947798	237
2	959	154	71964608	516
3	814	52	23869656	357
4	1030	85	52498328	465
5	368	40	3808314	194
6	354	67	5322988	217
7	332	44	2505523	169
8	367	48	3452574	188
9	519	62	6793956	235
10	551	60	7362516	241
11	1092	133	43055348	435
12	559	51	8345108	252
13	513	57	7491997	243
14	227	2	519373.6	100
15	431	46	4841927	210
16	500	83	8957392	258
17	495	50	6785424	235
18	499	56	5260008	216
19	444	43	4814164	210
20	414	54	4637069	207
21	296	40	2351715	165
22	393	79	5153589	214
23	329	44	3074541	180
24	483	51	5008449	212

Similarly, volumes were calculated for $NaNO_3$ particles representative of SSA from SOAS in Table S4. From these results, SSA particles were multiplied by a conversion factor of 0.67 to convert D_{pa} to D_{ve}.

Table S4. AFM-measured and volume-calculated diameters of NaNO3 particles impacted on silicon substrates, representative of SSA.

Particle #	D_{pa} (nm)	Height (nm)	Volume (nm^3)	D_{ve} (nm)
1	448	84	8981224	258
2	68	17	102174	58
3	171	29	821752	116
4	136	19	435493	94
5	100	13	205804	73
6	105	12	228540	76
7	250	58	2467066	168
8	258	77	2776954	174
9	153	29	648760	107
10	284	72	3454101	188
11	251	51	2288227	164
12	217	24	1243357	133
13	265	57	2718737	173
14	89	15	169364	69
15	320	67	4208101	200
16	745	108	24432611	360
17	273	55	2854158	176
18	217	40	1542059	143
19	458	79	8608666	254
20	199	33	1133683	129
21	319	69	4500131	205
22	383	64	5131053	214
23	187	9	676804	109
24	250	50	2184633	161

4 STXM-NEXAFS of a biological particle

STXM-NEXAFS was used to investigate the electronic properties and bonding nature of chemical species within carbon-containing particles since these particles were so prevalent at SOAS. The carbon K-edge was probed using this technique, and high spatial resolution information was obtained regarding carbonaceous particles. As SOA will be examined in detail using STXM-NEXAFS, only a primary biological particle is shown in Figure S2. From the NEXAFS spectrum (c), this particle contains C=C (285 eV), phenolic C (286.7 eV), and COOH (288.5 eV) functional groups (Moffet et al., 2010b;Moffet et al., 2010a;Solomon et al., 2005). The inorganic component was identified based on the absorbance of the pre-edge from 278 to 283 eV, which is offset compared to the post-edge region at 320 eV (Moffet et al., 2010a). The NEXAFS spectrum contains two sharp peaks at 297.1 and 299.7 eV characteristic of potassium. These features, along

with the oblong morphology, were used to identify the particle as biological (Moffet et al., 2010b). Although this particle also contains an sp^2 C inclusion, rather than soot the sp^2 C in the center of the particle is likely due to chlorophyll, a chelating porphyrin present within plant cells (Legall et al., 2007;Mauzerall, 1977).

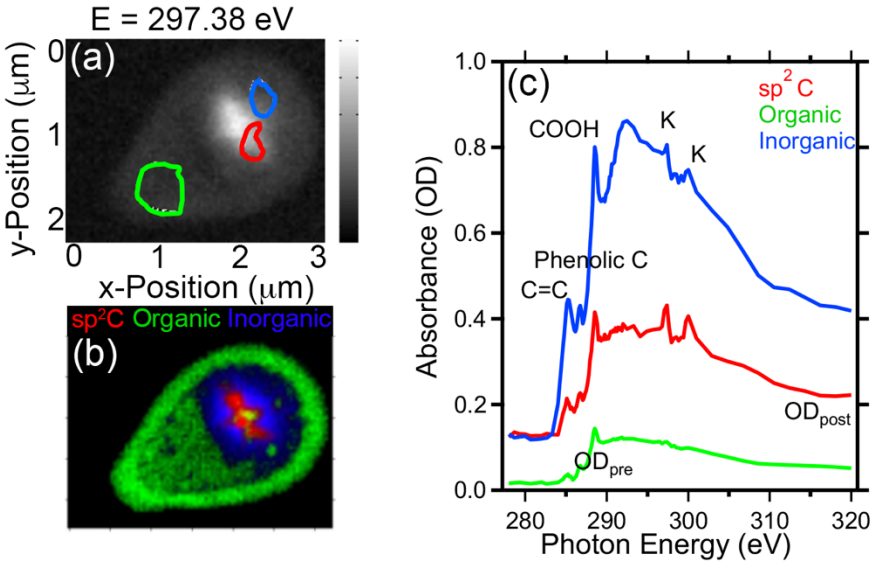

Figure S2. STXM-NEXAFS data of a primary biological particle. STXM images of the particles are shown in (a). Singular value decomposition maps combining sp^2 carbon (red), organic (green), and inorganic (blue) are depicted in (b). The NEXAFS spectrum for the particle at the carbon K-edge is shown in (c). Inorganic material was identified in both particles according to the pre-edge/post-edge offset.

5 Fresh soot calculation

Soot was difficult to detect using CCSEM-EDX due to interference from the Formvar B coating on the TEM grid. Therefore, the size distribution for soot was manually calculated from SEM images using samples on various stages from one day, and then a correction factor was applied to each sampling period based on the SEARCH network mass concentrations of elemental carbon (EC). This method likely overestimates the contribution of fresh soot since organic carbon/elemental carbon (OC/EC) SEARCH measurements include both fresh and aged soot, however the EC mass was used as an approximation of soot's contribution. To calculate the size distribution of soot particles during SOAS, all SEM images from July 9, 2013 4pm-7pm CST were

inspected for soot agglomerates. This sample was chosen for analysis because stages 7-11 of the MOUDI (0.056-0.56 μm 50% size cut; relevant sizes for soot) were available for imaging. Once a soot particle was identified, the particle was traced in ImageJ software to calculate the area. From this area, similar to the CCSEM software output, the projected area diameter (D_{pa}) was calculated and a size distribution using all soot D_{pa} was generated, shown below.

Table S5. Size distribution for fresh soot calculated for July 9, 2013 stages 7-11.

Projected Area Diameter (μm)	*Frequency*	*Fraction of soot per bin*
0.133352	0	0
0.177828	0	0
0.237137	5	0.065789474
0.316228	14	0.184210526
0.421697	27	0.355263158
0.562341	18	0.236842105
0.749894	11	0.144736842
1	0	0
1.333521	0	0
1.778279	1	0.013157895
2.371374	0	0
3.162278	0	0
4.216965	0	0
5.623413	0	0
7.498942	0	0
10	0	0
Total	76	

The fraction of soot per size bin was then used with the SEARCH network EC mass concentrations, measured using oxidative combustion, to calculate an approximate number of soot particles within each size range. First, the average EC mass was calculated for each time period of interest during SOAS. Then, the average $PM_{2.5}$ mass, measured using a tapered element oscillating microbalance (TEOM), was calculated for each time period. A scaling factor was generated by dividing EC mass/TEOM mass. The scaling factor calculated for each time period is: SOA (0.022), mineral dust (0.018), and SSA (0.029). This scaling factor was then multiplied by the size distributions in Table S5, giving results for the fraction of soot within the designated size bins for each of the three time periods.

6 Mass calculations and mixing state parameters

To calculate the mixing state parameters, atomic percentages were converted to mass fractions as described in the experimental section. To calculate elemental diversity, the mass of each element was used in the mixing state calculations shown below. To calculate mixing state due to aging during the SOA-rich, dust-rich, and SSA-rich time periods, elemental masses were assigned to specific source-based particle classes with the compositions described below. The elemental mass fractions for each of the three time periods are shown in Figure S3 depicting each element's contribution as a function of size. For the source-based elemental assignments, SOA particles consisted of solely S, biomass burning particles contained K and Cl, fly ash particles consisted of Si and Al, dust particles contained Na, Mg, Al, Si, K, Ca, Ti, and Fe, SSA particles contained Na, Mg, Cl, K, and Ca, and biological particles consisted of P, Cl, and K. Secondary species in this study were represented by S in every particle class, since organic (C, O) and nitrogen-containing species (N) are not quantitative using SEM-EDX (Laskin et al., 2006).

In addition to mass calculations, mixing state parameters were calculated for each elemental class to quantify diversity, and for the SOA, dust, and SSA time periods to quantify aging. The experimental section describes the equations used to calculate the entropy and mixing state index. Below are the definitions and equations for aerosol mass and mass fraction used to calculate the entropy along with equations for particle, species, and bulk population diversity (Riemer and West, 2013). The mass of species a in particle i is termed $\mu^a{}_i$ where $a = 1,\ldots, A$ and $i = 1,\ldots, N$. The total mass of particle i (μ_i) is given by

$$\mu_i = \sum_{a=1}^{A} \mu_i^a \quad (2)$$

The total mass of species a in the population (μ^a) is given by

$$\mu^a = \sum_{i=1}^{N} \mu_i^a \quad (3)$$

The total mass of the population (μ) is given by

$$\mu = \sum_{i=1}^{N} \mu_i \quad (4)$$

The mass fraction of species a in particle i ($p^a{}_i$) is given by

$$p_i^a = \frac{\mu_i^a}{\mu_i} \quad (5)$$

The mass fraction of particle i in the population (p_i) is given by

$$p_i = \frac{\mu_i}{\mu} \quad (6)$$

The mass fraction of species a in the population (p^a) is given by

$$p^a = \frac{\mu^a}{\mu} \quad (7)$$

The particle diversity of particle *i* (D_i) is given by

$$D_i = e^{H_i} \quad (8)$$

where H_i is the mixing entropy of particle *i*. The average particle species diversity (D_α) is given by

$$D_\alpha = e^{H_\alpha} \quad (9)$$

where H_α is the average particle mixing entropy. The bulk population species diversity (D_γ) is given by

$$D_\gamma = e^{H_\gamma} \quad (10)$$

where H_γ is the population bulk mixing entropy. D_α was used as a quantitative measure of elemental diversity for each particle class during SOAS (SOA, biomass burning particles, fly ash, dust, SSA, and biological particles.) However to quantify particle aging due to S during SOAS, the mixing state index (χ), a ratio between the average particle species diversity and bulk population species diversity, was calculated. While D_α is a useful metric to quantify elemental diversity, χ quantifies the degree of internal versus external mixing present within particle populations.

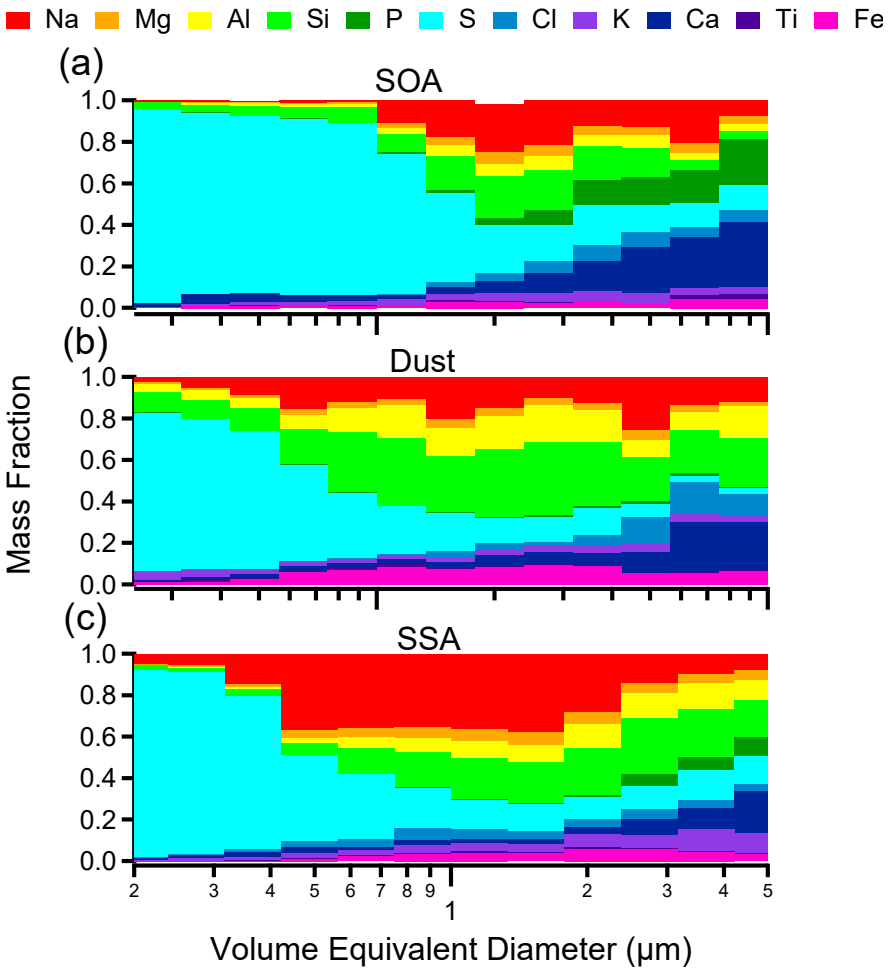

Figure S3. Mass fractions as a function of volume equivalent diameter for particle-rich time periods: (a) SOA-rich periods (June 14-17 and July 7-11, 2013), (b) dust-rich periods (June 12-13 and June 26-28, 2013), and (c) SSA-rich periods (June 10-11 and July 3-6, 2013.) C and O are not included in element quantification due to substrate interferences. *Only particles with a diameter between 0.2 - 5 μm are shown due to too few particles present at larger sizes for quantitative analysis.

7 STXM-NEXAFS soot identification

Two samples, June 10 and July 7, 2013, were analyzed using STXM-NEXAFS. In order to calculate the number fraction of particles from each sample that contained sp^2 C in the form of soot, matlab was used to visualize every particle in the sample. Each particle was screened on a per pixel basis for regions of high C=C content (> 35% C=C). If a pixel contained > 35 % C=C, then the script rendered a red pixel, stating that it was safe to call that region soot. The same was performed for the other colors (i.e. blue=inorganic, green=organic). Using this data, 6.9 % of

particles by number contained soot collected June 10, 2013 and 9.9 % of particles collected July 7, 2013 contained soot.

8 EDX of SOA on silicon

Most of the CCSEM-EDX analysis in this study was conducted on Formvar-coated TEM grids. However, since Formvar (a polymer) interferes with particle carbon and oxygen X-ray signals, additional EDX spectra of SOA particles were collected on Si substrates. EDX spectra from 61 particles (June 15, 2013 8pm-7am St. 8 sample) were collected and quantified with respect to C, N, O, and S. Figure S4 shows an example spectrum of an SOA/sulfate particle collected on Si. Note, the signal for Si extend beyond 80 counts, however the y-axis range shown here was selected to view the elements of interest (C, N, O, S). The average weight % of elements within SOA/sulfate from this analysis was 40 % C, 11 % N, 28 % O, and 20 % S. Though SOA/sulfate only contained 20% sulfur from this analysis, the mixing state indices for aerosol populations were calculated based on SOA/sulfate containing only sulfur, since CCSEM-EDX is not quantitative for C, N, and O.

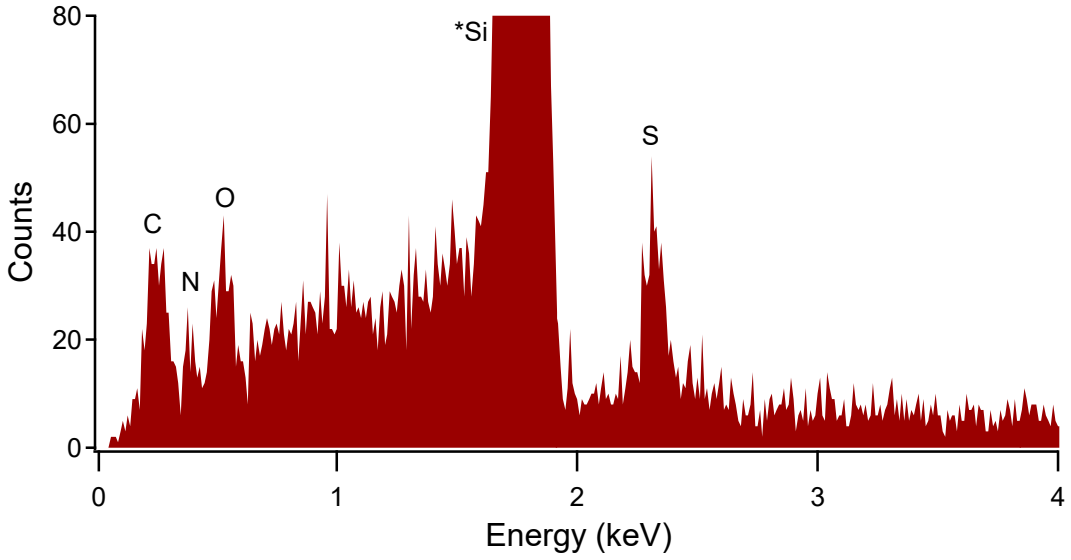

Figure S4. Example EDX spectrum of an SOA/sulfate particle collected on a silicon substrate.

9 Circularity equation

To determine the average circularity for SOA, biomass burning aerosol, and fly ash classes, the mode circularity was averaged across the k-means clusters assigned to that class in Equation 1:

$$C = 4\pi A/p^2 \quad (11)$$

where C is circularity, A is area of the particle, and p is the particle perimeter.

10 Nonvolatile cations

The number fraction of particles containing nonvolatile cations (Na, Mg, K, Ca, Fe) in sub- and supermicron sizes is shown in Figure S5 for the dust and SSA periods. In general, the number fraction of metal-containing particles is consistent for each class across the different periods (although there are minor differences between the sub- and super micron size ranges), suggesting that nonvolatile cations don't vary with processing, but are inherent to each class.

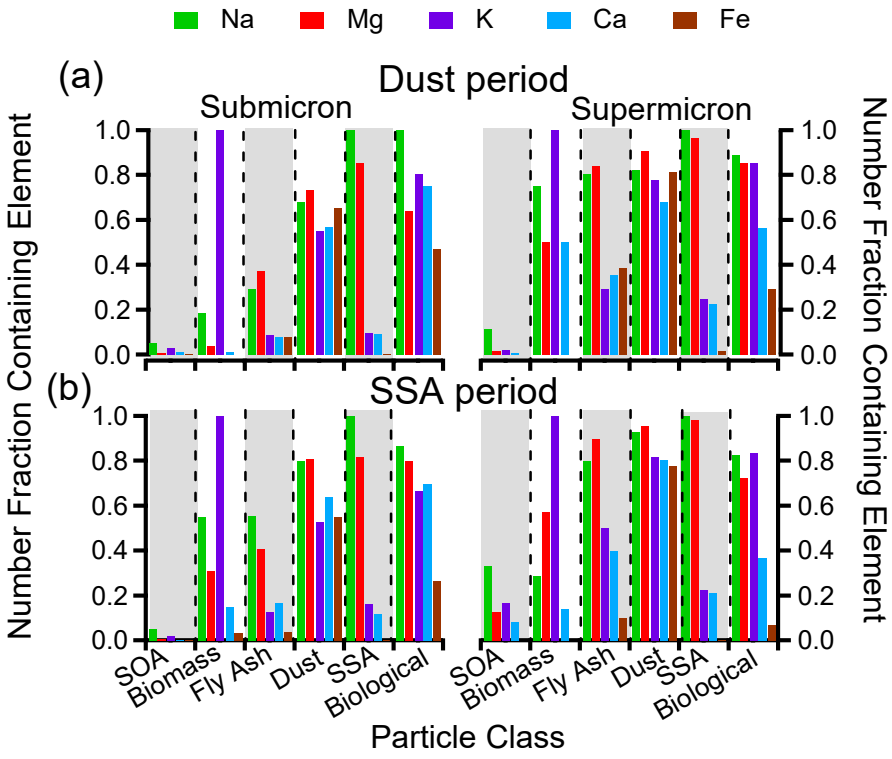

Figure S5. Size-resolved particle class compositions indicate the number fraction of particles in each class containing non-volatile cations Na, Mg, K, Ca, and Fe during the (a) dust period and (b) SSA period in the submicron and supermicron size range.

11 Significance of aging by sulfur during three events

The degree of secondary processing for each particle class was calculated as the average mass fraction of sulfur per particle (Figure S6). This parameter was used to calculate average sulfur diversity and along with the bulk population diversity, mixing state indices could be quantified. However, the mass fraction calculations here exclude C, N, and O since low Z elements are only semiquantitative with CCSEM. Excluding C, N, and O, SOA/sulfate have average sulfur mass fractions of 0.98 ± 0.08, 0.96 ± 0.13, 0.96 ± 0.16, during the SOA-influenced, dust-influenced, and SSA-influenced events, respectively. However, analysis of SOA on a non-carbonaceous substrate, which allowed C, N, and O to be quantified, demonstrated that the average mass fraction of sulfur

234 in SOA was actually 0.20 ± 0.04. This "actual" mass value for SOA was used to scale the average
235 mass fraction of sulfur for each period and is portrayed in Figure S6 by red markers. Using this
236 scaled mass fraction of sulfur, the "actual" mass of sulfur was 0.197 during the SOA-influenced
237 events, 0.193 during the dust periods, and 0.192 during the SSA periods.

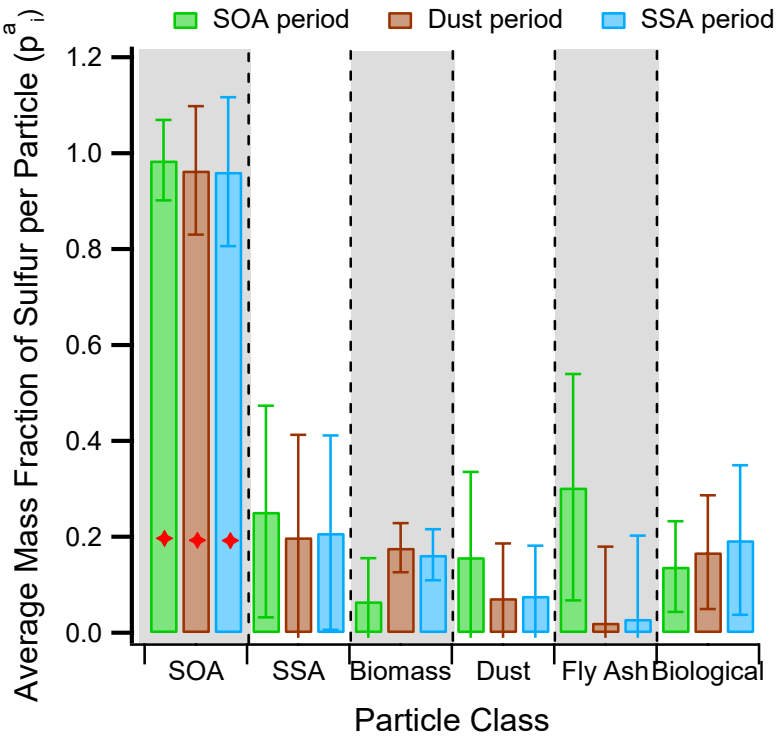

238

239 **Figure S6.** The secondary processing of particles by sulfate was calculated for each class during the three
240 time periods of interest as the average mass fraction of sulfur per particle. Red markers indicate the scaled
241 "actual" mass fraction of sulfur for SOA including mass contributions from C, N, and O.

242

243 A student's t-test was used to compare the average mass fraction of sulfur per particle for six main
244 particle classes (SOA/sulfate, biomass burning aerosol, fly ash, dust, SSA, and biological) during
245 the SOA events, dust events, and SSA events. The standard deviation, s_{pooled}, was calculated using
246 the following equation,

247 $$s_{pooled} = \sqrt{\frac{s_1^2(n_1-1)+s_2^2(n_2-1)}{n_1+n_2-2}} \quad (12)$$

where s_1 and s_2 are the standard deviations from the two samples, and n_1 and n_2 are the number of samples in each category. Then the student's t-test was calculated,

$$t_{calculated} = \frac{x_1 - x_2}{s_{pooled}} \sqrt{\frac{n_1 n_2}{n_1 + n_2}} \quad (13)$$

where x_1 and x_2 are the mean mass fraction of sulfur per particle class. The results of the student t-tests are located in Table S6, Table S7, and Table S8. The student's t-test was calculated to compare the aging of particle classes during the SOA vs. dust events, SOA vs. SSA events, and dust vs. SSA events. The difference in average sulfur mass fractions for all particle classes was found to be significant for the SOA vs. dust events and SOA vs. SSA events, but the difference was not statistically significant for the dust vs. SSA events at the 95% confidence interval.

Table S6. Student's t-test comparing average sulfur mass fractions among particle classes for the SOA vs. dust events

	SOA	Biomass	Fly Ash	Dust	SSA	Biological
x_1	0.985	0.260	0.070	0.169	0.306	0.140
x_2	0.964	0.177	0.022	0.072	0.199	0.168
s_1	0.081	0.221	0.091	0.179	0.235	0.096
s_2	0.134	0.214	0.051	0.114	0.156	0.119
s_{pooled}	0.095	0.048	0.006	0.128	0.194	0.099
degrees of freedom	120	120	120	120	120	120
$t_{calculated}$	10.97	3.95	5.67	19.82	13.49	2.50
95% CI t_{table}	1.98	1.98	1.98	1.98	1.98	1.98
significantly different?	yes	yes	yes	yes	yes	yes

Table S7. Student's t-test comparing average sulfur mass fractions among particle classes for the SOA vs. SSA events

	SOA	Biomass	Fly Ash	Dust	SSA	Biological
x_1	0.985	0.260	0.070	0.169	0.306	0.140
x_2	0.962	0.163	0.029	0.077	0.209	0.193
s_1	0.081	0.221	0.091	0.179	0.235	0.096
s_2	0.155	0.202	0.053	0.104	0.173	0.156
s_{pooled}	0.098	0.047	0.083	0.132	0.193	0.108
degrees of freedom	120	120	120	120	120	120
$t_{calculated}$	10.71	3.98	3.50	16.56	13.62	5.04
95% CI t_{table}	1.98	1.98	1.98	1.98	1.98	1.98
significantly different?	yes	yes	yes	yes	yes	yes

Table S8. Student's t-test comparing average sulfur mass fractions among particle classes for the dust vs. SSA events

	SOA	Biomass	Fly Ash	Dust	SSA	Biological
x_1	0.985	0.177	0.022	0.072	0.199	0.168
x_2	0.964	0.163	0.029	0.077	0.209	0.193
s_1	0.081	0.214	0.051	0.114	0.158	0.119
s_2	0.134	0.202	0.053	0.104	0.173	0.156
s_{pooled}	0.144	0.209	0.052	0.111	0.168	0.142
degrees of freedom	120	120	120	120	120	120
$t_{calculated}$	0.568	0.57	0.94	1.63	1.78	1.29
95% CI t_{table}	1.98	1.98	1.98	1.98	1.98	1.98
significantly different?	no	no	no	no	no	no

References

Bondy, A. L., Kirpes, R. M., Merzel, R. L., Pratt, K. A., Banaszak Holl, M. M., and Ault, A. P.: Atomic force microscopy-infrared spectroscopy of individual atmospheric aerosol particles: Subdiffraction limit vibrational spectroscopy and morphological analysis, Anal. Chem., 89, 8594-8598, 2017a.

Bondy, A. L., Wang, B., Laskin, A., Craig, R. L., Nhliziyo, M. V., Bertman, S. B., Pratt, K. A., Shepson, P. B., and Ault, A. P.: Inland sea spray aerosol transport and incomplete chloride depletion: Varying degrees of reactive processing observed during SOAS, Environ. Sci. Technol., 51, 9533-9542, 2017b.

Laskin, A., Cowin, J. P., and Iedema, M. J.: Analysis of individual environmental particles using modern methods of electron microscopy and X-ray microanalysis, J. Electron. Spectrosc. Relat. Phenom., 150, 260-274, 2006.

Marple, V. A., Rubow, K. L., and Behm, S. M.: A microorifice uniform deposit impactor (MOUDI)-description, calibration and use, Aerosol Sci. Technol., 14, 434-446, 1991.

Riemer, N., and West, M.: Quantifying aerosol mixing state with entropy and diversity measures, Atmos. Chem. Phys., 13, 11423-11439, 2013.